Westinghouse Non-Proprietary Class 3

CENPD-132 Supplement 4-NP-A,
Addendum 1-NP

May 2006

Calculative Methods for the CE Nuclear Power Large Break LOCA Evaluation Model

Improvement to 1999 Large Break LOCA EM Steam Cooling Model for Less Than 1 in/sec Core Reflood

Westinghouse

CENPD-132 Supplement 4-NP-A,
Addendum 1-NP

Calculative Methods for the CE Nuclear Power Large Break LOCA Evaluation Model

Improvement to 1999 Large Break LOCA EM Steam Cooling Model for Less Than 1 in/sec Core Reflood

Authors:

C. M. Molnar, Principal Engineer
Regulatory Compliance & Plant Licensing

E. F. Jageler, Jr.
Operations Analysis

R. B. Sisk, Manager
Fuel Engineering Licensing

Westinghouse Electric Company
Nuclear Fuel/Nuclear Services
4350 Northern Pike
Monroeville, PA 15146

This page intentionally left blank.

LEGAL NOTICE

COPYRIGHT NOTICE

This page intentionally left blank.

Table of Contents

Improvement to 1999 Large Break LOCA EM
Steam Cooling Model for Less Than 1 in/sec Core Reflood

This page intentionally left blank.

List of Figures

1999 Large Break LOCA Evaluation Model
Improvement to Steam Cooling Model for Less Than 1 in/sec Core Reflood

This page intentionally left blank.

1999 Large Break LOCA Evaluation Model
Improvement to Steam Cooling Model for Less Than 1 in/sec Core Reflood

1.0 Introduction

This report documents a change to the Appendix K steam cooling heat transfer component model in the Westinghouse 1999 Large Break Loss-of-Coolant Accident (LBLOCA) Evaluation Model (EM) for Combustion Engineering (CE) designed plants, Reference A.1, to include spacer grid heat transfer effects. This change is being implemented because of the consequences of Emergency Core Cooling System (ECCS) performance calculated using the 1999 EM for the CE 16x16 Next Generation Fuel (NGF) fuel design which are adversely impacted by the increase in core hydraulic pressure loss, the increase in core cross-sectional flow area, and the decrease in fuel rod cladding outside diameter. In particular, the core reflood calculations during a LBLOCA are adversely impacted by the changes in the core from CE 16x16 NGF implementation and the core reflood rates that are used to calculate reflood heat transfer coefficients for the hot rod are decreased. The CE 16x16 NGF design changes are estimated to have an insignificant impact on the ECCS performance peak cladding temperature. However, the impact of CE 16x16 NGF design changes on the ECCS performance maximum cladding local oxidation percentage for the hot rod rupture node is estimated to be large enough to warrant specific consideration.

CE 16x16 NGF design changes related to spacer grids impact evaluations using the 1999 EM for CE plants through the impact on hydraulic pressure loss. The 1999 EM does not have NRC-accepted spacer grid heat transfer models available for licensing calculations. Currently, there is no impact from CE 16x16 NGF design changes related to the details of the spacer grid design, placement, or potential impact on heat transfer other than through the core pressure drop change. Therefore, to improve ECCS performance calculated by the 1999 EM, a component model improvement has been made to include the effects of spacer grids. The component model improved is the 1999 EM steam cooling model for less than 1 in/sec core reflood. This improvement to the existing 1999 EM component model is intended to be an optional feature of the 1999 EM that is applicable to the CE 16x16 NGF design changes including Mid grids and Intermediate Flow Mixing (IFM) grids as well as to any other CE fuel design and will be used in future applications if deemed appropriate.

2.0 Description of 1999 EM Steam Cooling Model Change

2.1 Background

Spacer grids have an important effect on several key phenomena during the reflood period, including droplet breakup, interfacial heat transfer, and dispersed flow convective heat transfer. For the 1999 EM, these aspects of reflood heat transfer are covered by the use of the empirically-based, 10 CFR 50, Appendix K required, FLECHT correlation. The FLECHT correlation does not explicitly consider spacer grids, and is based on test measurements taken at mid-span locations, which are away from the direct effects of spacer grids. The FLECHT correlation, nevertheless, is considered here as having included the effects of spacer grids, even though the egg-crate grids used in those tests are not like the spacer grids for the CE 16x16 NGF assembly design.

As required by Appendix K for core reflood rates less than 1 in/sec, heat transfer calculations must be based on the assumption that cooling is only by steam. As described below, the 1999 EM component model for steam cooling on the rupture node and above for reflood rates less than 1 in/sec is being improved to include the effects of spacer grids, including IFM grids. This improvement is designed to more accurately model the steam flow rate and the steam cooling heat transfer coefficients on the hot rod rupture node and above. However to maintain a conservative bias for the impact of the improvement, the current Nuclear Regulatory Commission (NRC) specified EM constraint and limitation for this component model will be maintained; namely that, the 1999 EM steam cooling model for reflood rates less than 1 in/sec may not yield a heat transfer coefficient greater than determined by the FLECHT correlation.

2.2 1999 EM Steam Cooling Model for Core Reflood Rate Less Than 1 in/sec

The 1999 EM NRC-accepted steam cooling model is documented in Reference A.1 Section S III.D.6.b, Reference A.2, and Reference A.3, Section 2.7. To summarize its current configuration, the 1999 EM steam cooling model for core reflood rates less than (<) 1 in/sec is characterized by the following features and methodology constraints:

- The 1999 EM steam cooling model is an Appendix K required model, which is applied to the hot rod rupture node elevation and above when the core reflood rate is < 1 in/sec
- COMPERC-II reflood thermal-hydraulic calculations provide [ ]^{a,c}
- The steam cooling model includes [ ]^{a,c}
- HCROSS calculates single phase steam flow diversion from the hot rod rupture node blocked subchannel to unblocked adjacent subchannels; including flow recovery above the blockage
- PARCH calculates steam cooling heat transfer coefficients through the rupture node blockage and above; including the effect of steam superheating
- STRIKIN-II calculates rod-to-rod radiation heat transfer for the hot rod enclosure, which is also used by PARCH to calculate hot rod cladding temperatures needed for the steam cooling analysis

- The PARCH hot rod-to-coolant energy balance for calculating the steam temperature includes heat from cladding oxidation and decay heat
- The steam cooling model has imposed a FLECHT correlation upper bound that is required by an NRC-specified model constraint

2.3 Improved Model for Steam Cooling for Core Reflood Rate < 1 in/sec

The basis for the improved model for steam cooling includes no changes to the current model described above. An approach for improving the steam cooling heat transfer model has been developed utilizing the beneficial aspects of the CE 16x16 NGF spacer grids (both Mid grid and IFM grids) that are not included in the current model. The 1999 EM spacer grid improvements are patterned after models included in the Westinghouse BELOCA methodology (Reference A.4). The Westinghouse BELOCA spacer grid models have been NRC-accepted for and generically applied to many different spacer grid designs and fuel assembly lattice configurations. To summarize the improved model, the 1999 EM improved steam cooling model for core reflood rates < 1 in/sec includes the following features and methodology constraints:

- The revised steam cooling model considers only the spacer grids above the core two-phase level (both Mid grid and IFM grids)
- PARCH steam cooling heat transfer coefficients on the rupture node and above are augmented by the Westinghouse spacer grid heat transfer enhancement model, Reference A.4 Section 6-2-8
- Below the rupture node and above the core two-phase level, the steam flow rate [ ] a,c
- The FLECHT correlation upper bound required by NRC model constraint is also applied to the spacer grid model improvement, that is, the result of the grid model enhancement can not give a heat transfer coefficient greater than the FLECHT correlation
- Required physical characteristics of the Westinghouse spacer grid heat transfer enhancement model include
  - Maximum flow area reduction or spacer grid blockage fraction
  - Fuel lattice hydraulic diameter
  - Height of the spacer grid, used to estimate wetted surface area
  - Elevation of top edge of each spacer grid, relative to bottom of core

2.3.1 Basis for Improved Model

As described in Reference A.4, Sections 4-6-5 and 5-2-10, spacer grids are structural members of the fuel assembly, which support the fuel rods at a prescribed rod-to-rod pitch. With the exception of CE 16x16 NGF IFM grids in transition cores, all fuel assemblies have spacer grids at the same elevations across the core. Because the grids are at the same elevations, no flow bypass or flow redistribution occurs. Since the grid reduces the fuel assembly flow area, the flow is contracted and accelerated, and then expands downstream of each gridded layer in the core. As the flow is accelerated within the grid and then expands downstream, it re-establishes the thermal boundary layer on the fuel rod, which increases local heat transfer within and downstream of the grid. When the flow is a two-phase dispersed droplet flow, characteristic of PWR blowdown or reflood, the grids promote additional heat transfer effects. Since the grids are unpowered and have a large surface area to volume ratio, they quench before the fuel rods. When the grids quench, they create additional liquid surface area, which helps core cooling conditions by adding additional steam to the vapor stream by evaporation. Because the spacer grid blocks a portion of the fuel assembly flow area, the velocity of the vapor passing through the grid is higher than velocities nearby in the fuel bundle. As a result, the vapor-film relative velocity at the grid is larger, so that a wetted grid below the rupture node elevation has a higher interfacial heat transfer coefficient compared to nearby droplets. A thermal radiation heat transfer model is used to calculate the heat transfer from the adjacent fuel rods to the spacer grid:

[ ]a, c $(A-1)$

where

[ ]a, c

The temperature of the fuel rod in the above representation is taken to be the STRIKIN-II calculated cladding temperature of the average rod of the hot assembly on the axial node adjacent to the spacer grid. The average rod of the hot assembly is used instead of the hot rod, because the hot assembly average conditions are [

]a,c

In order to calculate the spacer grid temperature, the grid is [

]a,c.

That is,

[ ] ^{a,c} $(A-2)$

where

[ ] ^{a,c}

The grid temperature from this equation is

[ ] ^{a,c} $(A-3)$

The spacer grid heat transfer model provides [ ] ^{a,c} for use on the rupture node and above, when the reflood rate is < 1 in/sec. Only spacer grids located above the two-phase mixture level and below the rupture node elevation are used for this calculation and the spacer grid temperature must be less than the rewet temperature. That is,

[ ] ^{a,c} $(A-4)$

where

[ ] ^{a,c}

Several single-phase experiments show that the continuous phase heat transfer downstream of a spacer grid can be modeled on entrance effect phenomena where the abrupt contraction and expansion result in establishment of a new thermal boundary layer on the heated surface downstream of the grid. The entrance effect heat transfer decays exponentially downstream of the spacer grid and the local Nusselt number decreases exponentially downstream of the grid. Chiou, Hochreiter, and Young (1991)[A.5] summarized the single phase and two-phase experiments that demonstrated the grid convective enhancement effect, and provided a description of the effects of grids on the flow. [ ] ^{a,c}, which is given by:

[ ] a, c $(A-5)$

where

[ ] a, c

[ ] a,c

The convective heat transfer coefficient from the spacer grid to the vapor is represented by the Condie-Bengston IV correlation using a [ ] a,c The use of this correlation is consistent with the existing 1999 EM film boiling model in the CEFLASH-4A and STRIKIN-II codes (Reference A.3, Section 2.2 Equation (2.2.1-1)).

[ ] a, c $(A-6)$

where

[ ] a, c

Combining these two equations, where the spacer grid itself is located at Z = 0, the interfacial heat transfer coefficient for the wetted spacer grid becomes

[ ] a, c $(A-7)$

2.3.2 Improved Model as Coded

The emissivities of the fuel rod and spacer grid are given by the following from the PARCH code (Reference A.7, Section 3.4.1, Equation 3.4.1-5)

$$\left[\qquad \qquad \qquad \qquad \right]^{a,\,c} \qquad (A-8)$$

where

$$\left[\qquad \qquad \qquad \qquad \right]^{a,\,c}$$

The equivalent spacer grid cell diameter is defined as follows

$$\left[\qquad \qquad \qquad \qquad \right]^{a,\,c} \qquad (A-9)$$

where

P_{rod} = Assembly fuel rod pitch (ft)

The spacer grid liquid film interfacial surface area for heat transfer is estimated to be the grid metal surface area as follows:

$$A_{grid} = 4(P_{rod})H_{grid}N_{fuelrods} \qquad (A-10)$$

where

H_{grid} = Height of spacer grid (ft)
$N_{fuelrods}$ = Number of fuel rods in the core

The radiative heat flux to the spacer grid is calculated explicitly using the grid temperature from the previous time step. After the grid temperature for the current time step is calculated, the spacer grid temperature is numerically damped to prevent rapid changes as follows:

$$\left[\qquad \qquad \qquad \qquad \right]^{a,\,c} \qquad (A-11)$$

where

$$\left[\qquad \qquad \qquad \qquad \right]^{a,\,c}$$

The steam cooling convective heat transfer coefficients on the rupture node and above for reflood rates < 1 in/sec are based on the PARCH steam cooling model, as described above. To include the impact of the spacer grids on this heat transfer coefficient, the Westinghouse spacer grid heat transfer enhancement model is linearly averaged for the nodes located between spacer grid spans at and above the rupture node. This average representation is used because the PARCH and STRIKIN-II nodalizations are equal axial segments that are not specifically located with respect to the spacer grid locations. This nodalization is coordinated with the 1999 EM axial power shape methodology, which is characterized by axially dependent conditions selected for overall conservatism. Use of an average spacer grid enhancement model avoids continuity issues that would be introduced with an explicit axial dependent spacer grid model.

2.3.3 Impact of Improved Model

In most calculations with the 1999 EM, the limiting node for peak cladding temperature is generally either the FLECHT cooled node below the rupture node or the steam cooled node immediately above the rupture node. The limiting condition occurs during the time period of the transient when the core reflood rates are calculated to be < 1 in/sec. The rupture node is not usually the limiting node for peak cladding temperature. The impact of the improved steam cooling model for reflood rates < 1 in/sec based on spacer grid heat transfer effects is summarized as follows:

- Below the rupture node, the peak cladding temperature of the FLECHT cooled node is not impacted by the model changes with spacer grid heat transfer effects.
- Above the rupture node, the steam cooled node will experience a decrease in cladding temperature due to implementing the spacer grid heat transfer model effects. Figure A-1 shows this effect on the calculated cladding temperature for the node above the rupture node beginning after roughly 250 seconds. These results are a representative example of the performance of the revised model due to the spacer grid effects. The change in heat transfer coefficient at this elevation above the rupture node is shown in Figure A-2. Note that before 250 seconds in Figure A-2, the FLECHT heat transfer coefficients bound the steam cooling heat transfer coefficients. The magnitude of the reduction in cladding temperature depends on the plant-specific spacer grid arrangement and physical characteristics.
- On the rupture node, for the heat transfer conditions where the steam cooling heat transfer model is being used, the spacer grid model improves the heat transfer coefficient and lower rupture node temperatures are calculated.
- On the rupture node, when the FLECHT heat transfer coefficients are relatively low, the heat transfer calculation is limited by FLECHT and the steam cooling model may not be used. In this case, the spacer grid heat transfer model increases the time interval of FLECHT heat transfer being used to cool the rupture node until such time when the steam cooling heat transfer coefficient becomes less than the FLECHT heat transfer coefficient. This increased time interval for FLECHT cooling also lowers the calculated rupture node temperatures. Figure A-3 shows this effect beginning after roughly 300 seconds in the example case. The change in heat transfer coefficient on the rupture node

is shown in Figure A-4. The magnitude of the reduction in cladding temperature depends on the plant-specific spacer grid arrangement and physical characteristics.

- On all nodes, lower temperatures lead to lower calculated local cladding oxidation percentages. The magnitude of the reduction in maximum cladding local oxidation depends on the plant-specific spacer grid arrangement and physical characteristics.

3.0 Conclusion

An improvement is made to the 1999 EM steam cooling model for < 1 in/sec core reflood rates by utilizing the beneficial aspects of the CE 16x16 NGF spacer grids (both Mid grid and IFM grids). The amount of evaporated liquid that is calculated for the steam flow rate is increased by [

] a,c Increasing the steam flow rate leads to improved steam cooling heat transfer coefficients on the rupture node and above provided the FLECHT correlation is not more limiting. The spacer grid model is fundamentally based and applied in an overall conservative manner. The impact of the improved model will depend on the spacer grid arrangement and physical characteristics, which will be reflected in the plant-specific results of the full-core analyses.

4.0 References

A.1. CENPD-132P Supplement 1, "Calculational Methods for the C-E Large Break LOCA Evaluation Model," February 1975.

A.2. LD-81-095 Enclosure 1-P-A, "C-E ECCS Evaluation Model, Flow Blockage Analysis," December 1981.

A.3. CENPD-132 Supplement 4-P-A, "Calculative Methods for the CE Nuclear Power Large Break LOCA Evaluation Model," March 2001.

A.4. WCAP-12945-P-A, Volume 1 (Revision 2) and Volumes 2 through 5 (Revision 1), "Code Qualification Document for Best Estimate LOCA Analysis," March 1998.

A.5. WCAP-10484-P-A, "Spacer Grid Heat Transfer Effects During Reflood," March 1991.

A.6. Yao, S. C., Hochreiter, L. E., and Leech, J. J., 1982, "Heat Transfer Augmentation in Rod Bundles Near Grid Spacers," J. Heat Transfer, Vol. 104, pp. 76-81.

A.7. CENPD-138-P, "PARCH, A FORTRAN-IV Digital Program to Evaluate Pool Boiling, Axial Rod and Coolant Heatup," August 1974.

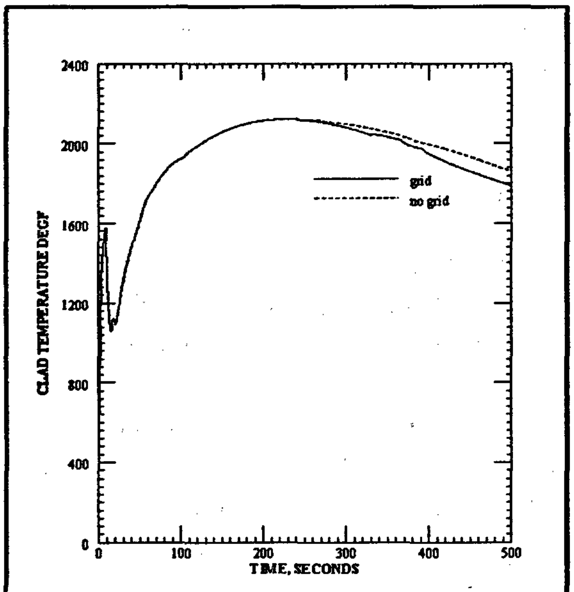

CLAD TEMPERATURE
Node 14 (Above Rupture Node)
Figure A-1

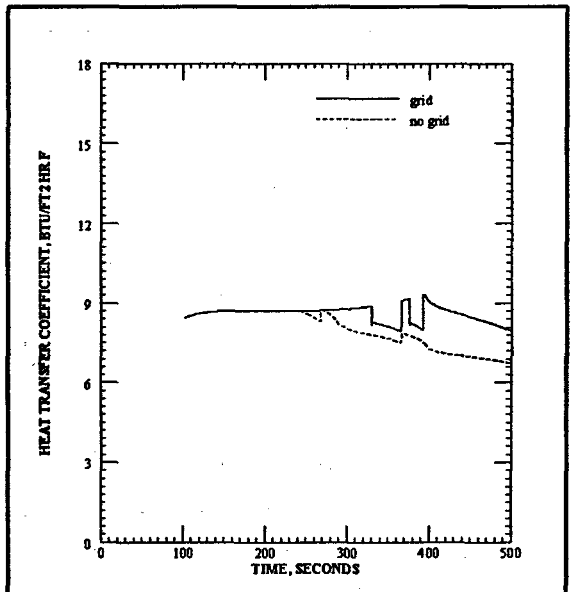

HEAT TRANSFER COEFFICIENT
Node 14 (Above Rupture Node)
Figure A-2

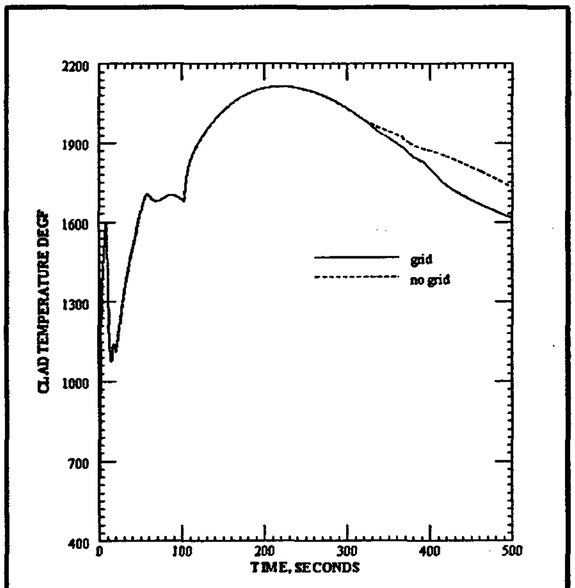

CLAD TEMPERATURE
Node 13 (Rupture Node)
Figure A-3

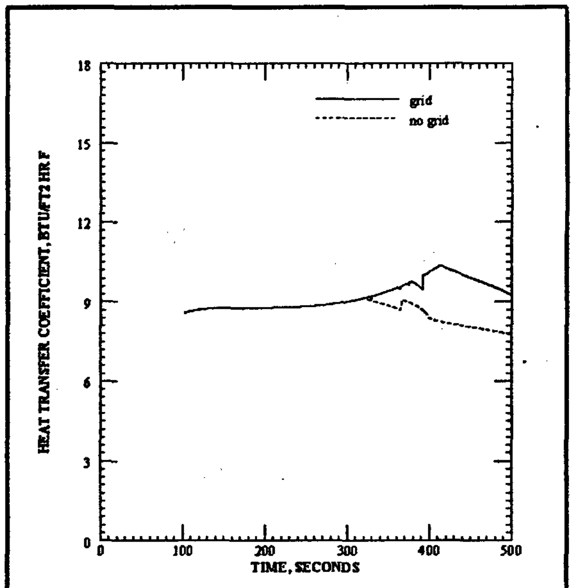

HEAT TRANSFER COEFFICIENT
Node 13 (Rupture Node)
Figure A-4